Oxidation of 4-Chlorobiphenyl Metabolites to Electrophilic Species by Prostaglandin H Synthase

ARTICLE *in* CHEMICAL RESEARCH IN TOXICOLOGY · JANUARY 2009

Impact Factor: 3.53 · DOI: 10.1021/tx800300t · Source: PubMed

Published in final edited form as:
Chem Res Toxicol. 2009 January ; 22(1): 64–71. doi:10.1021/tx800300t.

Oxidation of 4-chlorobiphenyl metabolites to electrophilic species by prostaglandin H synthase

Orarat Wangpradit[†,‡], **Lynn M Teesch**[§], **S. V. Santhana Mariappan**[€], **Michael W Duffel**[‡], **Karin Norstrom**[⊥], **Larry W Robertson**[†,‡], and **Gregor Luthe**[†,‡,£,*]

[†]*Department of Occupational and Environmental Health, University of Iowa, Iowa City, IA, USA* [‡]*Interdisciplinary Graduate Program in Human Toxicology, University of Iowa, Iowa City, IA, USA* [§]*High Resolution Mass Spectrometry Facility, University of Iowa, Iowa City, IA, USA* [€]*Central High-Field NMR Research Facility, Department of Chemistry, University of Iowa, Iowa City, IA, USA* [||]*College of Pharmacy, University of Iowa, Iowa City, IA, USA* [⊥]*Seamans Center for the Engineering Art and Sciences, University of Iowa, Iowa City, IA, USA* [£]*Institute of Life Sciences, Saxion University of Applied Sciences, Enschede, The Netherlands*

Abstract

Hormonally–sensitive tissues, like the prostate, ovary and breast, increasingly studied as targets of environmental chemicals, are sources of an enzyme potentially capable of transforming and activating xenobiotics to highly reactive metabolites. Our study specifically addresses the question of whether prostaglandin H synthase (PGHS) can activate phenolic metabolites of polychlorinated biphenyls (PCBs). We found that human recombinant PGHS-2 catalyzed the oxidation of *ortho* (2′, 3′-, 3′,4′-) and *para* (2′,5′-) dihydroxy 4-chlorobiphenyl metabolites to their corresponding quinones. These were trapped *in situ* with N-acetyl cysteine and the reaction products were isolated and characterized by liquid chromatography coupled mass spectrometry and ^{1}H and heteronuclear (^{1}H-^{13}C) nuclear magnetic resonance spectroscopy. Both mono- and di-N-acetyl cysteine Michael addition adducts were identified, with the 2′,3′-, and 2′,5′-dihydroxy metabolites predominantly forming mono-N-acetyl cysteine adducts, while the 3′,4′-dihydroxy predominantly formed di-substituted N-acetyl cysteine adducts. These studies clearly demonstrate that the phenolic metabolites of these environmental pollutants are activated by PGHS, as co-substrates, to highly reactive electrophilic PCB quinones, with a potential for protein and DNA damage, especially in non-hepatic tissues where the enzyme is found.

Introduction

Since Silent Spring (1), a keen interest has developed in the occurrence and environmental health impacts of persistent environmental pollutants, like the polychlorinated biphenyls (PCBs). Large reserves of these halogenated pollutants are found throughout the world (2). We lack a clear mechanistic understanding of their toxicity. Traditional approaches have focused on the liver, as a target organ, and on the regulation and catalytic properties of the cytochrome P-450 (CYP) superfamily, abundant there (3). More recently, hormonally - sensitive tissues, such as the prostate, ovary and breast, have become of increasing interest as targets of toxicity. These organs are a source of a unique xenobiotic – metabolizing enzyme, known as prostaglandin H synthase (PGHS) (4,5). PGHS is a bi-functional enzyme, containing both cyclooxygenase and peroxidase activities (6,7) and is up-regulated by several xenobiotics (8,

*To whom correspondence should be addressed: phone +1 319 335 4221, fax +1 319 335 4290, E-mail: gregor-luthe@uiowa.edu

9). Hydroxylated PCB (OH-PCB) metabolites resulting from oxidative metabolism catalyzed by CYPs in the liver and other tissues (10,11) may enter the blood stream and are distributed to all organs and tissues. Indeed PCBs have been suggested as risk factors for cancer development in prostate (12,13) ovary (14,15) and breast (16,17).

Previous studies have demonstrated DNA damage occurring during PCB metabolism in the presence of peroxidases (*i.e.* horseradish peroxidase, myeloperoxidase, and lactoperoxidase with the formation of DNA adducts, oxidized DNA bases and strand breaks (17-20). The oxidation of catechol and hydroquinone metabolites of PCBs to yield semiquinones, and subsequently quinones, is a proposed mechanism for the formation of these highly reactive electrophilic species. Quinone metabolites of 4-chlorobiphenyl (4-CB) were observed in qualitative UV-VIS studies to interact with nitrogen and sulfur nucleophiles and with DNA. Both Michael-addition and radical mechanisms have been suggested for the adduct formations (21).

Bioactivation of several estrogens and catechols to quinones with the formation of sulfhydryl adducts was previously studied in microsomes (22-25). Although PGHS has a peroxidase component, it is not immediately clear that PGHS has the ability to transform hydroxylated non planar substrates, like PCB metabolites, into highly reactive quinones.

In the present study we tested the hypothesis that hydroxylated PCBs (OH-PCBs) **(2-5)**, such as those originating from CYP-catalyzed oxidative metabolism, may function as co-substrates during the oxidation of arachidonic acid to prostaglandins in reactions catalyzed by PGHS, thereby transforming the OH-PCBs **(2-5)** into highly reactive electrophilic quinoid PCB species **(6-8)** that are capable of reacting with nucleophilic sites on nucleic acids and proteins. Such modifications of cellular macromolecules may contribute to various toxic responses, including carcinogenesis (17,20,26). We have now studied human recombinant PGHS-2 (hPGHS-2) with *ortho*- (2′,3′- **(3)**, 3′,4′- **(4)**) and *para*- (2′,5′- **(5)**) dihydroxy-4-CB as model substrates and have identified the *N*-acetyl cysteine (NAC)-adducts of the quinone metabolites **(6-8)** by liquid chromatography coupled mass spectrometry (LC-MS) and nuclear magnetic resonance spectroscopy (NMR).

Experimental Procedures

Materials

4-Chlorobiphenyl (4-CB **(1)**) was purchased from EGA-Chemie, Germany. 4′-Hydroxy-4-chlorobiphenyl (4-CB-4′-OH **(2)**) was purchased from TCI America (Portland, OR). 2′,3′-Hydroxy-4-chlorobiphenyl (4-CB-2′,3′-OH **(3)**), 3′,4′-hydroxy-4-chlorobiphenyl (4-CB-3′,4′-OH **(4)**), 2′,5′-hydroxy-4-chlorobiphenyl (4-CB-2′,5′-OH **(5)**), and 4-chlorobiphenyl-2′,5′-benzoquinone (4-CB-2′5′-Q **(8)**) were synthesized as described (27) and provided by Drs. Luthe and Lehmler. 4-Chlorobiphenyl-2′,3′-benzoquinone (4-CB-2′,3′-Q **(6)**), and 4-chlorobiphenyl-3′,4′-benzoquinone -(4-CB-3′,4′-Q **(7)**) were obtained by oxidation of 4-CB-2′, 3′-OH, and 4-CB-3′,4′-OH using silver oxide as described by Espandiari *et al* (11). The purities of 4-CB-2′3′-Q **(6)** and 4-CB-3′,4′-Q **(7)** were determined by proton nuclear magnetic resonance spectrometry (^{1}H NMR). 3-Fluoro-4-chlorobiphenyl-2′,5′-benzoquinone (3-F-4-CB-2′,5′-Q **(9)**) was synthesized according to the method of Amaro *et al*. (21) (70% yield, 99% purity). The internal standard, 3′-NAC-3-fluoro-4-chlorobiphenyl-2′,5′-benzoquinone (3-F-4-CB-2′,5′-Q-3′-NAC **(10)**) was synthesized by adding dropwise 1 mmol NAC solution to 1 mmol of 3-F-4-CB-2′,5′-Q **(9)** dissolved in dimethyl sulfoxide (DMSO). The reaction was continuously stirred for 20 minutes. The adduct was purified by high performance liquid chromatography (HPLC) using 2.1 mm i.d. × 15 cm, 5 μm Supelco Discovery C-18 column (Sigma Aldrich, MO). The mobile phase was 0.1% formic acid in water (A) and 0.1% formic acid in acetonitrile (B). The fractions were freeze-dried and rediluted in deuterated water for

purity determination by ^{1}H NMR (yield 27%, purity 99%). hPGHS-2, arachidonic acid (AA), 5-bromo-2[4-fluorophenyl]-3-[4-methylsulfonylphenyl]- thiophene (DuP-697), and PGHS inhibitor screening assay kit (catalog number 560131) were purchased from Cayman chemical company (Ann Arbor, MI). Hematin (MP biomedicals, Solon, OH), NAC (Acros organics, Sommerville, NJ), and solvents and reagents (Fisher Chemical, Chicago, IL) were purchased from the sources indicated.

Methods

PGHS-2 inhibitor screening with model compounds (1-5)—The PGHS-2 inhibitor test applying EIA technique (28,29) for the model compounds (Fig.1), 4-CB **(1)**, 4-CB-4′-OH **(2),** 4-CB-2′,3′-OH **(3)**, 4-CB-3′,4′-OH **(4)**, and 4-CB-2′,5′-OH **(5)**, was conducted using PGHS inhibitor screening assay kit from Cayman chemical (30). The selective PGHS-2 inhibitor, DuP-697 (31), at 5 nM was used in the assay to determine the relative inhibitor effects as positive control. The concentration of prostaglandin $F_{2\alpha}$ ($PGF_{2\alpha}$) formed in each well was calculated from the absorbance.

Incubation of di-hydroxy-PCBs (3-5) with hPGHS-2—The assay mixture was developed from Marnett *et al*. (32-34). The mixture contained 100 mM potassium phosphate buffer (pH 7.4), 100 μM potassium arachidonate (KAA), 1 μM hematin, 50 μM NAC, 50 μM of the model compounds **(3-5)** as substrates, and 100 units of hPGHS-2 in a 1 mL total reaction volume. Activity levels were defined as described by the manufacturer: one unit is the amount of enzyme capable of consuming 1 nmol of oxygen per minute at 37 °C in prostaglandin biosynthesis. 3-F-4-CB-2′,5′-Q-3′-NAC **(10)**, at 50 μM, was used as the internal standard for all reactions. Stock solutions of 100 μM hematin, 5 mM internal standard, and 5 mM substrates, 4-CB-2′,3′-OH **(3)**, 4-CB-3′,4′-OH **(4)**, and 4-CB-2′,5′-OH **(5)**, were diluted in DMSO while 10 mM KAA and 5 mM NAC were diluted in ultrapure water. KAA was prepared *in situ* by adding 100 μmol of AA to react with 100 μmol of potassium hydroxide. The reactions were initiated by the addition of KAA to the solution containing hPGHS-2, hematin, NAC, and substrates, and terminated by the addition of 50 μL of 1N hydrochloric acid after incubation in the shaker bath at 37 °C for 0, 1, 5, 10, and 15 minutes. 3-F-4-CB--2′,5′-Q-3′-NAC **(10)** was added to each reaction immediately before terminating the reaction. Reactions with inactive hPGHS-2 prepared by heating at 80 °C for 10 minutes, and reactions without KAA were used as controls. After reactions were terminated, the reaction mixtures were transferred to 10KDa Amicon Ultracentrifugal filters from Millipore (Billerica, MA) and centrifuged in an Eppendorf 5810R (Hamburg, Germany) at 2,000g for 20 minutes. The filtrates were collected and transferred to 2mL amber vials. Oxygen in all samples was minimized by degassing the samples under argon for 10 minutes. Samples were kept at −20 °C before identification and quantification with LC-MS. Peak area of each analyte was normalized by the area of 3-F-4-CB-2′,5′Q-3′-NAC **(10)** (35,36).

Product identification and quantification by LC-MS—Analysis of the incubation mixtures was performed on a ThermoFinnigan LCQ deca (Thermo Scientific, San Jose CA). Chromatographic separations were performed at 25°C on a 2.1 mm i.d. × 15 cm, 5 μm Supelco Discovery C-18 column coupled to Supelguard column, 2.1 mm i.d. × 2 cm, 5 μm (Sigma-Aldrich, MO). The mobile phases used were 0.1% formic acid in water (A) and 0.1% formic acid in acetonitrile (B) delivered at a total flow rate of 200 μL/min. The gradient profile was programmed as follow: 65 % A: 35% B isocratic held from 0 to 2 mins gradient B up to 100% from 2 to 30 mins. The samples were injected using a 200-vial autosampler equipped with a 50 μL loop. The LC was coupled with a photo diode array (PDA) detector followed by mass spectrometer (MS) operated in positive electrospray ionization (ESI) mode. The detection wavelengths were 254 nm for channel A, and 280 nm for channel B of the PDA. MS data were acquired over single ion monitoring (SIM) mode at *m/z* ranges of 379.5-382, 397.5-400,

540.5-543, and 558.5-561. The SIM *m/z* ranges were selected from *m/z* values of the calibration standards (379.9, 381.9, 540.9, and 542.9), and the internal standard (397.9, 399.9, 558.9, and 560.9) at 50 μM preliminarily determined over full scan mode (*m/z* 200-700).

Sample preparation and characterization by NMR—The repeated fraction collection of the products was conducted using a 5 μm Supelco Discovery C-18 column, 2.1 mm i.d. × 15 cm, equipped with UV detector at 290 nm. The column temperature was programmed at 25°C. Mobile phases and gradient were adjusted as described in the previous section but the injection volume was changed to 100 μL. Each product fraction was collected ten times at the retention time that its UV spectrum has shown the highest intensity. After collection, all products were dried thoroughly with a freeze-dryer overnight to complete dryness and re-diluted in deuterated solvents for nuclear magnetic resonance experiments. All products were characterized by the Avance-300 and Avance-600 Bruker NMR spectrometers (Billerica, MA) operating at 300 and 600 MHz respectively using deuterated methanol (CD_3OD) as solvent. Deuterated chloroform was used as solvent for quinones. ^1H and ^{13}C chemical shifts were referenced (37) with the residual proton and carbon chemical shifts of the solvents (CD_3OD, ^1H, 3.31 ppm, ^{13}C, 49.15 ppm; $CDCl_3$, ^1H, 7.27 ppm). Fractions with milligram quantities of the product were characterized with a battery of one- and two-dimensional heteronuclear experiments (^1H, 1D-COSY, 1D-TOCSY, NOESY, ^{13}C, ^{13}C-DEPT, HMQC, and HMBC). Gradient-assisted versions of the pulse sequences and inverse detection (38) were used for these 2D experiments. Typical parameters for the NMR experiments were as follows: ^1H (TD, 64k; NS, 4k), ^{13}C (TD, 128k; NS, 10000), ^{13}C-DEPT (TD, 128k; NS, 5000), 1D-COSY (TD, 64k; NS, 512), 1D-TOCSY (TD, 64k; NS, 512), NOESY (TD, 2k; TD1, 256; NS, 32; DS, 32; mixing times, 1.0, 1.5, and 2.0s), ^{13}C-^1H-HMQC (TD, 2k; TD1, 128; NS, 32; DS, 128); ^{13}C-^1H-HMBC (TD, 2k; TD1, 128; NS, 32; DS, 128). TD, NS and DS refer to time domain data points, number of scans and dummy scans respectively. All the NMR data were processed with TOPSPIN 1.3 suite of software programs. One-dimensional ^1H data were processed with zero-filling to 64k data points and 0.2 Hz exponential line broadening, whereas ^{13}C spectra were processed with zero-filling to 128k data points and 1.0 Hz of exponential line broadening. The two-dimensional NMR data were processed with the zero-filling to 2048 points and 1024 points in acquisition and second dimension respectively. Relative numbers of proton signals multiplied by the integral areas were used for the quantification (39). Simple ^1H NMR analysis was only performed, when a fraction contains a single metabolite in sub-milligram levels or a fraction contains a mixture of metabolites resulting in complex NMR spectra.

Results

In an initial experiment we examined the potential for model hydroxylated-PCBs (Fig. 1) to serve as co-substrates for hPGHS-2 using an EIA quantifying the $PGF_{2\alpha}$ formed after treatment of the reaction product, prostaglandin H_2 (PGH_2), with stannous chloride. This analysis showed the biphasic nature of PCB metabolism catalyzed by PGHS where specific di-hydroxy-PCBs stimulated the formation of PGH_2. Parent PCB 3

(1) and mono-hydroxy-PCB 3 **(2)** inhibited this reaction, see Figure 2. With increased concentrations of **(1,2),** the formation of $PGF_{2\alpha}$ was diminished. The di-hydroxy-PCBs **(3-5)** on the other hand functioned as substrates. The substrate activity of 4-CB-2′,3′-OH **(3)** was 30-40% higher compared with 4-CB-3′,4′-OH **(4)** and 4-CB-2′,5′-OH **(5)** which exhibited similar values. Increased substrate concentrations **(3-5)** resulted in exponentially increased $PGF_{2\alpha}$ formation.

We tested the model compounds **(3-5)** in an *in vitro* enzyme assay as co-substrates using hPGHS-2. NAC was used as trapping agent. Aliquots of reaction mixtures were taken at five

incubation time points (*i.e.*, 0, 1, 5, 10, and 15 min). Identification and quantification of intermediates and products were performed by LCESI-MS (Table 1) and NMR spectroscopy (Table 2), using a F-tagged analogue of the NAC adduct 3-F-4-CB-2′,5′-Q-3′-NAC **(10)**, as an internal standard (35). The LC-ESIMS method did not lead to fragmentations, but exhibited $[M+H]^+$ ion patterns of monochlorinated analytes as the major signals in the spectrum. The *m/z* values of the quinonemono-NAC adducts were 381.9 and 383.9, quinone-di-NAC adducts were 543.0 and 545.0, where as 4-CB-2′,5′-Q-di-NAC also exhibited an ion at *m/z* 540.9.

Off-line LC fractions were collected, the solvent exchanged for deuterated methanol for the NMR characterization of the NAC-adducts. Though eight fractions of the PCB-NAC adducts were studied by NMR spectroscopy, ^{1}H and ^{13}C resonance assignments were made only for mono- NAC adducts of 4-CB-3′,4′-OH and 4-CB-2′,5′-OH. Further analyses are required for other fractions, since their ^{1}H spectra are complex either due to the coexistence of multiple populations and or due to microgram quantities of the material (Figure 3). Figure 4 shows the ^{1}H aromatic and peptide spectral regions, and HMBC cross-section of the 4-CB-3′,4′-OH-5′-NAC. 1D TOCSY data established the J-coupling networks of the aromatic and NAC portions of the adduct, whereas the HMBC data is compatible with the NAC substituted at the C5′ position; long-range ^{1}H-^{13}C correlation peaks were observed between β-H_2 of NAC and PCB portion of the adduct, and between the two aromatic rings. The observed ^{1}H-^{1}H J-coupling constants are also compatible with the proposed structure of the NAC-adduct. However, the observed 1D ^{1}H, and ^{13}C, and the 2D heteronuclear NMR data can also be explained by 4-CB-3′,4′-OH-6′-NAC, an isomeric form of the C5′-NAC, where the NAC is linked at the C6′ position instead of C5′. The distances of H2-H2′ (2.76A), H2-H6′ (4.22A), H6-H2′ (4.23A), and H6-H6′ (2.75A) for C5′-NAC and H2-H2′ (3.05A), H2-H5′ (5.61A), H6-H2′ (3.93A), and H6-H5′ (5.06A) for C6′-NAC computed with the structures built and energy minimized (Spartan molecular modeling package) and the NOESY data collected at mixing times 1.0, 1.5, and 2.0s (NOEs are observed for the resonance at 7.53ppm with the resonances at 7.17ppm and at 7.01ppm) support the formation of C5′-NAC adduct. A distance of 2.75A is expected to generate a strong NOE between the resonances at 7.53ppm and 7.17ppm, where as a distance of 5.06A is expected to generate no or very weak NOE. Similar results were also observed for 4-CB-2′,5′-OH-4′-NAC. Table 2 lists the ^{1}H and ^{13}C chemical shifts of 4-CB-3′,4′-OH-6′-NAC and 4-CB-2′,5′-OH-4′-NAC. The OH-signals of the di-hydroxy products could not be identified; a fast exchange of the proton with the deuterium of the MeOD was expected. The NMR analyses was also performed for 3-F-4-CB-2′,5′-Q (IS) and NAC, as a reference to the substrates investigated. The ^{1}H and ^{13}C chemical shifts of IS were confirmed by homonuclear and heteronuclear 2D NMR data (published elsewhere). The diastereotropic $CH_{2\beta}$ protons of NAC assume the strong coupling case ($|\nu_{\beta 2}- \nu_{\beta 1}| \sim |5J_{\beta 1\_\beta 2}|$) with further spliting from the CH_α. On the contrary, $CH_{2\beta}$ protons of NAC from C5′-NAC generate well-resolved dd patterns.

Figure 5 shows the formation of mono- and di-NAC adducts after trapping of the quinoid PCBs: 4-CB-2′,5′-OH **(8)** (Figure 5A) **(A)**, 4-CB-2′,3′-OH **(6)** (Figure 5B), and 4-CB-3′,4′-OH **(7)** (Figure 5C). All concentrations were normalized to the applied internal standard. Blanks were determined using hPGHS-2 that had been inactivated by denaturation. A major difference between the transformation of the three isomers is that 4-CB-2′,3′-OH **(3)**, and 4-CB-2′,5′-OH **(5)** predominantly form mono-NAC adducts while the 4-CB-3′,4′-OH **(4)** predominantly resulted in di-substituted NAC adducts.

Discussion

In the h-PGHS 2 enzyme immunoassay, the parent PCB 3 **(1)** and mono-hydroxyPCB 3 **(2)** inhibited this reaction, while the di-hydroxy-PCB metabolites **(3-5)** functioned as substrates, acting as activators of AA metabolism. The di-hydroxy PCB model compounds **(3-5)** functioned as electron donors and were oxidized to quinones **(6-8)**, while prostaglandin G_2

(PGG_2), was reduced to PGH_2. The increased substrate specificity of 4-CB-2′,3′-OH **(3)** can be explained on the basis of the redox potentials of the *ortho*-**(4,5)** and the *para*-isomer **(3)** (21). A higher redox potential is thermodynamic favorable.

The results of the enzyme immunoassay prompted us to carry the testing of our hypothesis further with an independent second method of the co-substrates **(3-5)** in an hPGHS-2 *in vitro* assay in the presence of the nucleophilic trapping agent NAC. This provided a technique for the detection of the highly reactive electrophilic quinoid PCB metabolites formed *in situ*. We found that the model di-hydroxy metabolites **(3-5)** were transformed into quinones. The quinones **(6-8)** reacted with NAC by a Michael addition. Aromatization by enol-keto-tautomerism resulted in NAC-substituted di-hydroxy analogues, that underwent further oxidation and nucleophilic addition, see Figure 6. The quantification was done using the concept of F-tagged analogues as internal standards that has proven to be an outstanding tool. F-tagged analogues exhibit a close similarity in their physical-chemical behavior but are easily to distinguish by NMR and/or MS (36) The differences in the transformation of the di-hydroxy substrates **(3-5)** in their ability to form di-NAC adducts is most likely due to the positive mesomeric effect of the 3′,4′-dihydroxy metabolite enhancing a second nucleophilic addition. No tri-NAC substituted 4-CB-quinones were detected. The di-NAC-adducts of 4-CB-2′,3′-Q **(6)** and 4-CB-3′,4′-Q **(7)** did not allow a further nucleophilic addition since there was no β-position available. For 4-CB-2′,5′-Q-di-3′,4′-NAC, the 6′-position was still available but not strongly electrophilic. Therefore, only a great excess of NAC may compel the formation of 4-CB-2′,5′-Q-tri-3′,4′,6-NAC, but was not observed.

As summarized in Figure 2, PGHS-2 catalyzed the transformation of di-hydroxyPCB metabolites **(3-5)** into highly reactive electrophilic quinones **(6-8)**, which reacted rapidly with nucleophilic NAC. Among the possible consequences of reaction of electrophilic quinones derived from PCBs with nucleophiles may be covalent binding to cellular macromolecules and subsequent initiation of carcinogenic or other toxic responses. The specific roles of PGHS-catalyzed oxidation of PCB metabolites in toxic responses to PCBs remain to be elucidated, but these results point to mechanisms of activation prevalent in non-hepatic tissues such as prostate, ovary, and breast.

Acknowledgments

We thank Hans-Joachim Lehmler for providing several study compounds. The research was made possible by grants ES013661 and ES05605 from the National Institute of Environmental Health Sciences, and by the Alexander von Humboldt Foundation, Bonn, Germany. Its contents are solely the responsibility of the authors and do not necessarily represent the official views of the granting agencies.

Abbreviations

PGHS, prostaglandin H synthase
hPGHS-2, human recombinant PGHS type 2
PCBs, polychlorinated biphenyls
CYP, cytochrome P-450
NAC, *N*-acetyl cysteine
ESI, electrospray ionization
SIM, single ion monitoring
LC-ESI-MS, liquid chromatography coupled electron spray ionization mass spectrometry
COSY, correlated spectroscopy
TOCSY, total correlation spectroscopy
NOESY, nuclear Overhauser Effect Spectroscopy
HMQC, heteronuclear multiple quantum coherence
HMBC, heteronuclear multiple bond correlation

DEPT, distortionless enhancement by polarization transfer
OH-PCB, hydroxylated PCBs
PCB 3; 4-CB, 4-chlorobiphenyl
4-CB-4′-OH, 4′-hydroxy-4-chlorobiphenyl
4-CB-2′,3′-OH, 2′,3′-dihydroxy-4-chlorobiphenyl
4-CB-3′,4′-OH, 3′,4′-dihydroxy-4-chlorobiphenyl
4-CB-2′,5′-OH, 2′,5′-dihydroxy-4-chlorobiphenyl
4-CB-2′,5′-Q, 4-chlorobiphenyl-2′,3′-benzoquinone
4-CB-3′,4′-Q, 4-chlorobiphenyl-3′,4′-benzoquinone
4-CB-3′,4′-Q, 4-chlorobiphenyl-2′,5′-benzoquinone
3-F-4-CB-2′,5′-Q, 3-fluoro-4-chlorobiphenyl-2′,5′-benzoquinone
3-F-4-CB-2′-5′-Q-3′-NAC, 3′-NAC-3-fluoro-4-chlorobiphenyl-2′,5′-benzoquinone
AA, arachidonic acid
KAA, potassium arachidonate
PGG_2, prostaglandin G2
PGH_2, prostaglandin H2
$PGF_{2\alpha}$, prostaglandin $F2_{\alpha}$
DMSO, dimethyl sulfoxide
DuP-697, 5-bromo-2[4-fluorophenyl]-3-[4-methylsulfonylphenyl]- thiophene
EIA, enzyme immunoassay

References

1. Carson, R. Silent Spring. Houghton Mifflin; Boston: 1962.
2. Fiedler, H. Global and local disposition of PCBs. In: Robertson, LW.; Hansen, LG., editors. Recent Advances in Environmental Toxicology and Health Effects. University Press of Kentucky; Lexington, KY: 2001. p. 11-15.
3. Ludewig, G.; Esch, .; Robertson, LW. Polyhalogenierte Bi- und Terphenyle, Chapter 20. In: Dunkelberg, H.; Gabel, T.; Hartwig, A., editors. Handbuch der Lebensmitteltoxikologie. Wiley-VCH Weinheim; Germany: 2007. p. 1031-1094.
4. Vogel C, Boerboom AM, Baechle C, El-Bahay C, Kahl R, Degen GH, Abel J. Regulation of prostaglandin endoperoxide H synthase-2 induction by dioxin in rat hepatocytes: possible c-Src-mediated pathway. Carcinogenesis 2000;21:2267–2274. [PubMed: 11133817]
5. Smith WL, DeWitt DL, Garavito RM. Cyclooxygenases: structural, cellular, and molecular biology. Annu Rev Biochem 2000;69:145–182. [PubMed: 10966456]
6. Kurumbail RG, Kiefer JR, Marnett LJ. Cyclooxygenase enzymes: catalysis and inhibition. Curr. Opin. Struc. Biol 2001;11:752–760.
7. Malkowski MG, Ginell SL, Smith WL, Garavito RM. The productive conformation of arachidonic acid bound to prostaglandin synthase. Science 2000;289:1933–1937. [PubMed: 10988074]
8. Brant K, Caruso RL. Late-gestation rat myometrial cells express multiple isoforms of phospholipase A2 that mediate PCB 50-induced release of arachidonic acid with coincident prostaglandin production. Toxicol. Sci 2005;88:222–230. [PubMed: 16120751]
9. Bezdecny SA, Roth RA, Ganey PE. Effects of 2,2′,4,4′-tetrachlorobiphenyl on granulocytic HL-60 cell function and expression of cyclooxygenase-2. Toxicol. Sci 2005;84:328–334. [PubMed: 15673847]
10. McLean MR, Bauer U, Amaro AR, Robertson LW. Identification of catechol and hydroquinone metabolites of 4-monochlorobiphenyl. Chem. Res. Toxicol 1996;9:158–164. [PubMed: 8924585]
11. Espandiari P, Glauert HP, Lehmler HJ, Lee EY, Srinivasan C, Robertson LW. Initiating activity of 4-chlorobiphenyl metabolites in the resistant hepatocyte model. Toxicol. Sci 2004;79:41–46. [PubMed: 14976334]
12. Prince MM, Ruder AM, Hein MJ, Waters MA, Whelan EA, Nilsen N, Ward EM, Schnorr TM, Laber PA, Davis-King KE. Mortality and exposure response among 14,458 electrical capacitor

manufacturing workers exposed to polychlorinated biphenyls (PCBs). Environ. health Persp 2006;114:1508–1514.

13. Ritchie JM, Vial SL, Fuortes LJ, Guo H, Reedy VE, Smith EM. Organochlorines and risk of prostate cancer. J. Occup. Environ. Med 2003;45:692–702. [PubMed: 12855910]
14. Ptak A, Ludewig G, Lehmler HJ, Wojtowicz AK, Robertson LW, Gregoraszczuk EL. Comparison of the actions of 4-chlorobiphenyl and its hydroxylated metabolites on estradiol secretion by ovarian follicles in primary cells in culture. Reprod. Toxicol 2005;20:57–64. [PubMed: 15808786]
15. Ptak A, Ludewig G, Kapiszewska M, Magnowska Z, Lehmler HJ, Robertson LW, Gregoraszczuk EL. Induction of cytochromes P450, caspase-3 and DNA damage by PCB3 and its hydroxylated metabolites in porcine ovary. Toxicol. Lett 2006;166:200–211. [PubMed: 16949219]
16. Lin CH, Lin PH. Induction of ROS formation, poly(ADP-ribose) polymerase-1 activation, and cell death by PCB126 and PCB153 in human T47D and MDA-MB-231 breast cancer cells. Chem. Biol. Interact 2006;162:181–194. [PubMed: 16884709]
17. Oakley GG, Devanaboyina U, Robertson LW, Gupta RC. Oxidative DNA damage induced by activation of polychlorinated biphenyls (PCBs): implications for PCB-induced oxidative stress in breast cancer. Chem. Res. Toxicol 1996;9:1285–1292. [PubMed: 8951230]
18. Oakley GG, Robertson LW, Gupta RC. Analysis of polychlorinated biphenyl-DNA adducts by 32P-postlabeling. Carcinogenesis 1996;17:109–114. [PubMed: 8565118]
19. McLean MR, Robertson LW, Gupta RC. Detection of PCB adducts by the 32P-postlabeling technique. Chem. Res. Toxicol 1996;9:165–171. [PubMed: 8924587]
20. Srinivasan A, Lehmler HJ, Robertson LW, Ludewig G. Production of DNA strand breaks in vitro and reactive oxygen species in vitro and in HL-60 cells by PCB metabolites. Toxicol. Sci 2001;60:92–102. [PubMed: 11222876]
21. Amaro AR, Oakley GG, Bauer U, Spielmann HP, Robertson LW. Metabolic activation of PCBs to quinones: reactivity toward nitrogen and sulfur nucleophiles and influence of superoxide dismutase. Chem. Res. Toxicol 1996;9:623–629. [PubMed: 8728508]
22. Moridani M, Scobie H, Salehi P, O'Brien PJ. Catechin Metabolism: Glutathione conjugate formation catalyzed by tyrosinase, peroxidase and cytochrome P450. Chem. Res. Toxicol 2001;14:841–848. [PubMed: 11453730]
23. Iverson SL, Shen L, Anlar N, Bolton JL. Bioactivation of estrone and its catechol metabolites to quinoid-glutathione conjugates in rat liver microsomes. Chem. Res. Toxicol 1996;9:492–499. [PubMed: 8839054]
24. McGirr LG, Subrahamanyam VV, Moore GA, O'Brien PJ. Peroxidase-catalyzed 3-(gluatathion-S-yl)-p,p′-biphenol formation. Chem. Biol. Interact 1986;60:85–99. [PubMed: 3779886]
25. Josephy PD, Iwaniw DC. Identification of the N-acetylcysteine conjugate of benzidine formed in the peroxidase activation system. Carcinogenesis 1985:155–158. [PubMed: 3967336]
26. Pereg D, Tampal N, Espandiari P, Robertson LW. Distribution and macromolecular binding of benzo [a]pyrene and two polychlorinated biphenyl congeners in female mice. Chem. Biol. Interact 2001;137:243–258. [PubMed: 11566292]
27. Bauer U, Amaro AR, Robertson LW. A new strategy for the synthesis of polychlorinated biphenyl metabolites. Chem. Res. Toxicol 1995;8:92–95. [PubMed: 7703372]
28. Van Weemen BK, Schuurs AH. Immunoassay using antigen-enzyme conjugates. FEBS Lett 1971;15:232–236. [PubMed: 11945853]
29. Engvall E, Perlman P. Enzyme-linked immunosorbent assay (ELISA). Quantitative assay of immunoglobulin G. Immunochemistry 1971;8:871–874. [PubMed: 5135623]
30. Cayman chemical, Ann Arbor, MI. EIA workshop. Ann arbor, MI: 2002. EIA.
31. Gans KR, Galbraith W, Roman RJ, Haber SB, Kerr JS, Schmidt WK, Smith C, Hewes WE, Ackerman NR. Anti-inflammatory and safety profile of DuP 697, a novel orally effective prostaglandin synthesis inhibitor. J. Pharmacol. Exp. Ther 1990;254:180–187. [PubMed: 2366180]
32. Marnett LJ, Johnson JT, Bienkowski MJ. Arachidonic acid-dependent metabolism of 7,8-dihydroxy-7,8-dihydro-benzo[a]pyrene by ram seminal vesicles. FEBS Lett 1979;106:13–16. [PubMed: 499485]

33. Marnett LJ, Bienkowski MJ. Hydroperoxide-dependent oxygenation of trans-7,8-dihydroxy-7,8-dihydro benzo[a]pyrene by ram seminal vesicle microsomes. Source of the oxygen. Biochem. Biophys. Res. Commun 1980;96:639–647. [PubMed: 7191704]

34. Marnett LJ, Rowlinson SW, Goodwin DC, Kalgutkar AS, Lanzo CA. Arachidonic acid oxygenation by COX-1 and COX-2. Mechanisms of catalysis and inhibition. J. Biol. Chem 1999;274:22903–22906. [PubMed: 10438452]

35. Luthe, G.; Ariese, F.; Brinkman, U. A. Th. Monofluorinated Polycyclic Aromatic Hydrocarbons : Standards in Environmental Chemistry and Biochemical Applications. In: Neilson, AH., editor. Handbook of Environmental Chemistry : Organic Fluorine Compounds. Springer Verlag; Berlin, Germany: 2002. p. 249-275.

36. Luthe G, Garcia-Boy R, Jacobus J, Smith B, Rahaman A, Robertson LW, Ludewig G. Xenobiotic Geometry and Media pH determine Cytoroxicity though solubility. Chem. Res. Toxicol 2008;21:1017–1027. [PubMed: 18402468]

37. Gottlieb HE, Kotlyar V, Nudelman A. NMR Chemical Shifts of Common Laboratory Solvents as Trace Impurities. J. Org. Chem 1997;62:7512–7515. [PubMed: 11671879]

38. Gunther, H. NMR Spectroscopy : Basic principles, Concepts, and Applications in Chemistry. Vol. 2nd Edition. John Wiley & Sons; New York: 1995.

39. Tyszka JM, Fraser SE, Jacobs RE. Magnetic resonance microscopy: recent advances and applications. Curr. Opin. Biotech 2005;16:93–99. [PubMed: 15722021]

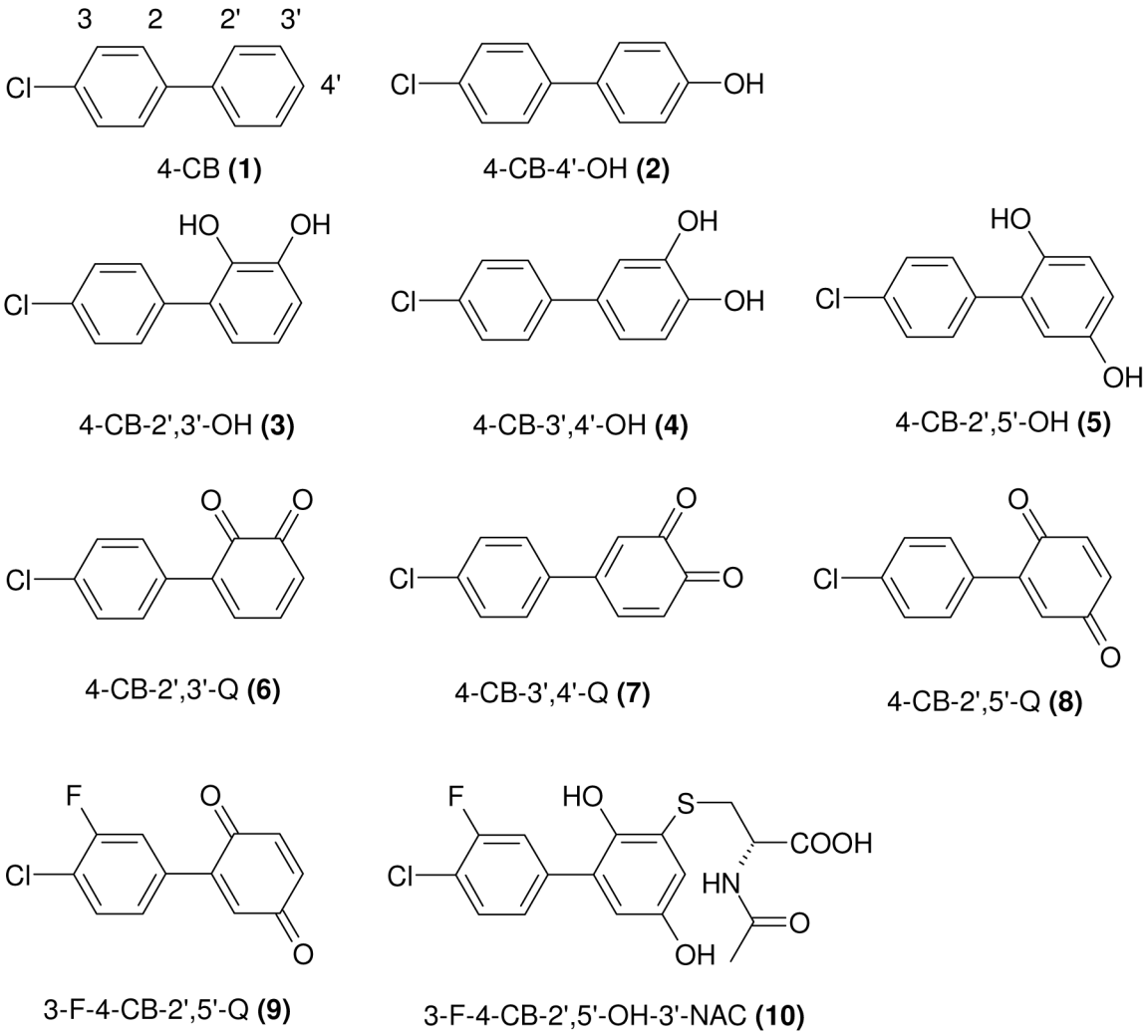

Fig. 1.
Structures of the compounds used in this study. The numbers in brackets are used as the structure references in this report.

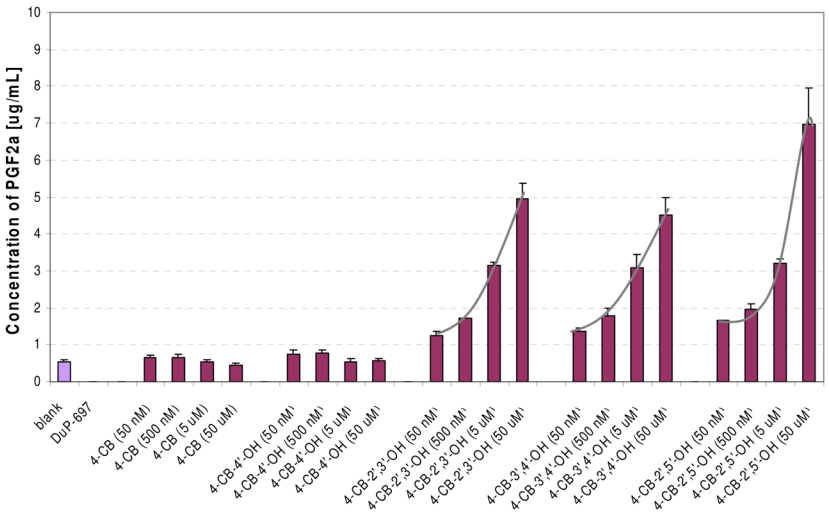

Fig. 2.

PGHS-2 inhibitor screening assay shows the concentration [μg/mL] of $PGF_{2\alpha}$ bound to rabbit antiserum for blank, DuP-697, and the model compounds, 4-CB **(1)**, 4-CB-4′-OH **(2)**, 4-CB-2′, 3′-OH **(3)**, 4-CB-3′,4′-OH **(4)**, and 4-CB-2′,5′-OH **(5)**, at 50 nM, 500 nM, 5 μM, and 50 μM. Value shown are average (n=3) with standard deviations.

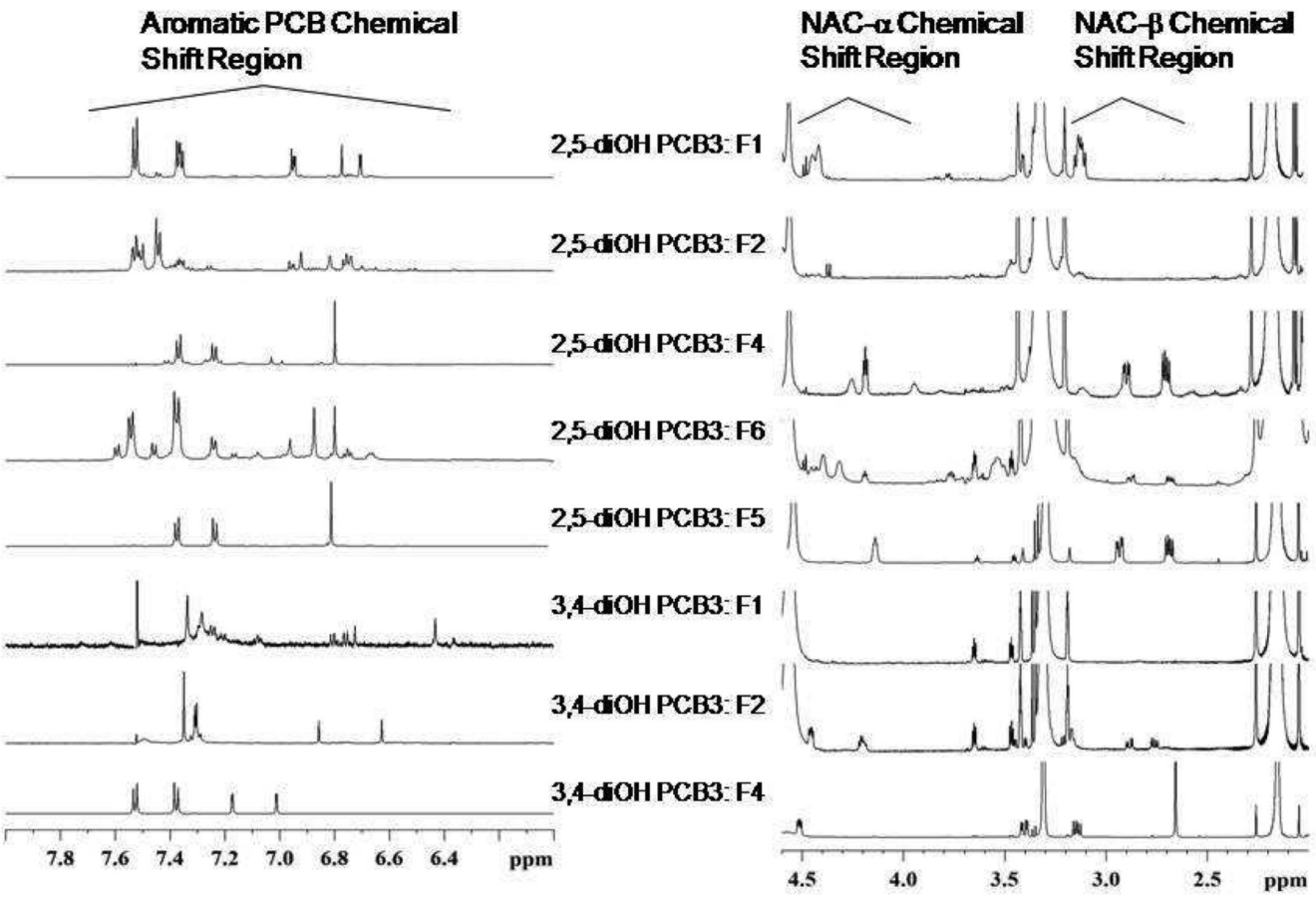

Fig. 3.

^{1}H aromatic and peptide (NAC-α, NAC-β) spectral regions of different fractions (F) of 4-CB-2′, 5′-OH-NAC and 4-CB-3′,4′-OH-NAC.

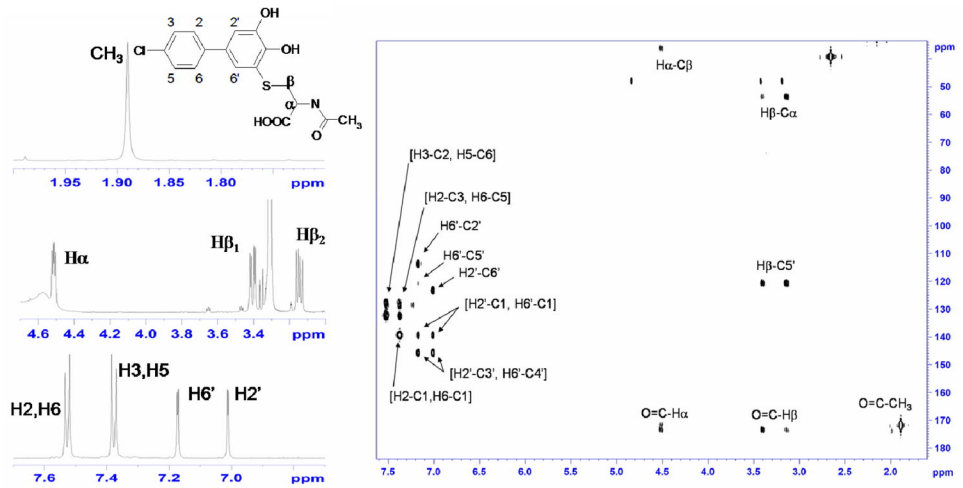

Fig. 4.

^{1}H aromatic and peptide spectral regions, and HMBC cross-section of 4-CB-3′,4′-OH-5′-NAC. 1D TOCSY data established the J-coupling networks of the aromatic and NAC portions of the adduct, whereas the HMBC data is compatible with the NAC substituted at the C5′ position; long-range ^{1}H-^{13}C correlation peaks can be observed between β-H_2 of NAC and PCB portion of the adduct, and between the two aromatic rings. NOE data also supported the formation of C5′-NAC adduct.

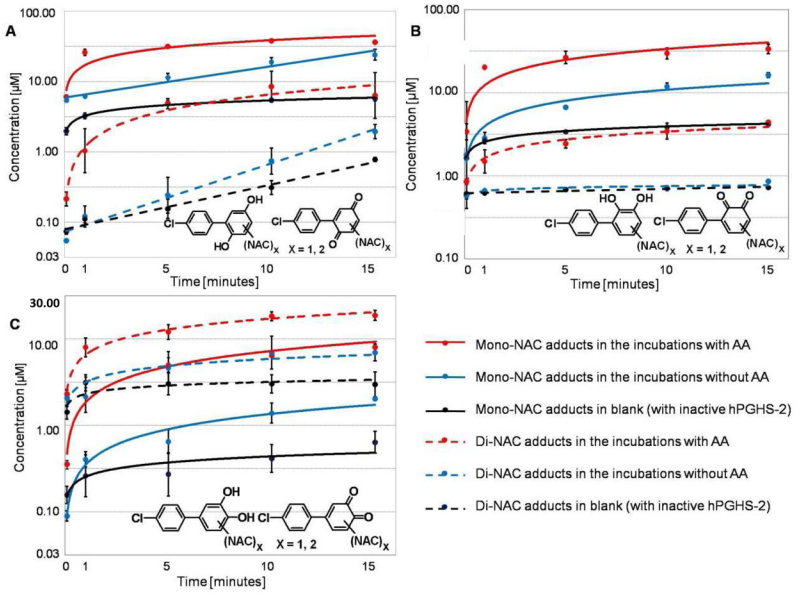

Fig. 5.

Concentration of mono- and di-NAC adducts of quinones and hydroquinones formed in the incubation of 4-CB-2′,5′-OH **(8)** (Figure A), 4-CB-2′,3′-OH **(6)** (Figure B), and 4-CB-3′,4′-OH **(7)** (Figure C) with hPGHS-2 at 0, 1, 5, 10, and 15 minutes.

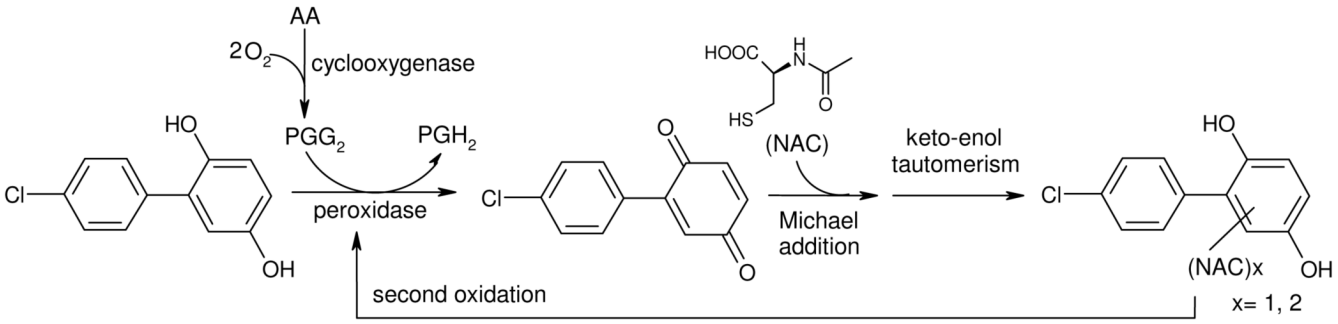

Fig. 6.

Summary of the proposed mechanism of PGHS-2-catalyzed formation of PGH_2 by di-hydroxy-4-chlorobiphenyl with formation of a reactive electrophilic quinone. The quinone was trapped by the nucleophile *N*-acetylcysteine (NAC), rearranging by ketoenol tautomerism to a hydroquinone, that can serve again as substrate. AA: arachidonic acid, PGG_2: prostaglandin G_2, PGH_2: prostaglandin H_2, NAC: *N*-acetylcysteine.

Table 1

m/z values and relative abundance [%] of ions of 4-CB-benzoquinone-mono-NAC and 4-CB-benzoquinone-di-NAC adducts formed as the ultimate products from the incubation study using NAC as the trapping agent.

adducts	***m/z* values and relative abundance [%]**
4-CB-2′,3′-Q-$(NAC)_1$	$[M+H]^+$ *381.9* (100%), *383.9* (26%)
4-CB-2′,3′-Q-$(NAC)_2$	$[M+H]^+$ *543.0* (100%), *545.0* (54%)
4-CB-3′,4′-Q-$(NAC)_1$	$[M+H]^+$ *381.9* (100%), *383.9* (38%)
4-CB-3′,4′-Q-$(NAC)_2$	$[M+H]^+$ *543.0* (100%), *545.0* (46 %)
4-CB-2′,5′-Q-$(NAC)_1$	$[M+H]^+$ *379.8*, *381.9* (100%), *381.8*, *383.9* (38%)
4-CB-2′,5′-Q-$(NAC)_2$	$[M+H]^+$ *540.9*, *543.0* (100%), *542.8* (56%), *545.0* (44%)

Table 2

The ^{1}H NMR results of each compound are listed as chemical shifts, δ determined in ppm relative to TMS, and coupling constants, *J*, in Hz. 4-CB-benzoquinones are determined in $CDCl_3$ and NAC adducts in MeOD.

Compound	Chemical shifts δ [ppm] and $^{1}H^{1}H$, $^{1}H^{19}F$ couplings *J* [Hz]
3-F-4-CB-2′,5′-Q (IS)	6.85 (H3′, H4′, H6′, 3H, m), *δ 7.21* (H5, 1H, *ddd*, ^{3}J=8.3Hz, ^{4}J=2.1Hz, $^{5}J_{HF}$ =0.9Hz), *δ 7.32* (H2, 1H, *dd*, ^{3}J =9.9Hz, ^{4}J=2.1Hz), *δ 7.46* (H5, 1H, *dd*, $^{4}J_{HF}$=7.5Hz, ^{3}J=8.3Hz), *δ 117.6* (C2), *δ 123.3* (C4), *δ 125.5* (C6), *δ 130.8* (C5), *δ 133.1* (C6′), *δ 136.4* (C3′)*, *δ 137.0* (C4′)*, *δ 143.6* (C1′), *δ 157.1* (C1), *δ 158.7* (C3), *δ 185.9* (C5′)*, *δ 187.1* (C2′)*
N-acetyl-cysteine (NAC)	*δ 1.86* (CH3, 3H, *s*), *δ 2.86* ($CH2_{\beta}$(1), 1H, *dd*, ^{2}J=14.1Hz, ^{3}J=6.7Hz), *δ 2.94* ($CH2_{\beta}$(2), 1H, *dd*, ^{2}J=14.1Hz, ^{3}J=4.4Hz), *δ 4.59* (CH_{α}, 1H, overlapping dd, $^{3}J_{\beta1}$=6.9Hz, $^{3}J_{\beta2}$=4.6Hz)
4-CB-2′,5′-OH-4′-NAC	*δ 1.86* (CH3, 3H, *s*), *δ 2.69* ($CH2_{\beta}$ (1), 1H, *dd*, ^{2}J=13.5Hz, ^{3}J=7.2Hz), *δ 2.94* ($CH2_{\beta}$ (2), 1H, *dd*, ^{2}J=13.5Hz, ^{3}J=4.5Hz), *δ 4.16* (CH_{α}, 1H, broad t), *δ 6.80* (H-3′/6′, 2H, *s*), *δ 7.23* (H-2/6, 2H, *d*, ^{3}J=8.5Hz), *δ 7.36* (H-3/5, 2H, *d*, ^{3}J=8.4Hz), *δ 22.4* (CH3), *δ 38.2* (C_{β}), *δ 55.7* (C_{α}), *δ 116.1* (C3′), *δ 118.9* (C6′), *δ 119.0* (C4′), *δ 127.6* (C3, C5), *δ 132.3* (C2, C6), *δ 133.0* (C1′), *δ 136.0* (C4), *δ 147.8* (C5′), *δ 152.0* (C2′), *δ 172.6* (C=O, Aceto)
4-CB-3′,4′-OH-6′-NAC**	*δ 1.89* (CH3, 3H, *s*), *δ 3.15* ($CH2_{\beta}$ (1), 1H, *dd*, ^{2}J=13.8Hz, ^{3}J=7.9Hz), *δ 3.40* ($CH2_{\beta}$ (2), 1H, *dd*, ^{2}J=13.8Hz, ^{3}J=4.5Hz), *δ 4.51* (CH, 1H, dd, ^{3}J=7.9Hz, ^{3}J=4.5Hz), *δ 7.53* (H-2/6, 2H, *d*, ^{3}J=8.5Hz), *δ 7.38* (H-3/5, 2H, *d*, ^{3}J=8.5Hz), *δ 7.17* (H-6′, 1H, d, ^{5}J=2.1Hz), *δ 7.01* (H-2′, 1H, d, ^{5}J=2.1Hz), *δ 21.3* (CH3), *δ 36.2* (C_{β}), *δ 53.7* (C_{α}), *δ 113.6* (C2′), *δ 120.7* (C5′), *δ 123.1* (C6′), *δ 127.6* (C2, C6), *δ 128.4* (C3, C5), *δ 132.5* (C4), *δ 139.4* (C1), *δ 145.8* (C3′, C4′)), *δ 171.8* (C=O, Aceto)

* tentative due to similar chemical environments.

** C1′ is too weak to identify